



# Volcanosonda: A Novel, Lightweight and Low-Cost Instrument for In-Situ Characterization of Volcanic Clouds – A Cross-Comparison Experiment

Camilo Naranjo<sup>1</sup>, Marcello Bitetto<sup>2</sup>, Maria Fabrizia Buongiorno<sup>1</sup>, Ernesto Corrales<sup>3</sup>, Jorge Andres Diaz<sup>3,4</sup>,  
5 Alessandro Filippeschi<sup>5</sup>, Matteo Gemignani<sup>5</sup>, Gaetano Giudice<sup>6</sup>, Lorenzo Guerrieri<sup>1</sup>, Irene Marsili<sup>5</sup>, Luca  
Merucci<sup>1</sup>, Malvina Silvestri<sup>1</sup>, Dario Stelitano<sup>1</sup>, Angelo Vitale<sup>2</sup>, Riccardo Biondi<sup>7</sup>, Salvo Marcuccio<sup>5</sup>, Stefano  
Corradini<sup>1</sup>

<sup>1</sup>Istituto Nazionale di Geofisica e Vulcanologia (INGV), ONT, Rome, Italy

10 <sup>2</sup>Università di Palermo, Dipartimento di Scienze della Terra e del Mare (DiSTeM), Palermo, Italy

<sup>3</sup>Universidad de Costa Rica (UCR), GasLab, CICANUM, San José, Costa Rica

<sup>4</sup>INFICON Inc., East Syracuse, New York, USA

<sup>5</sup>University of Pisa, Space Systems Laboratory, Dept. of Civil and Industrial Engineering, Pisa, Italy

<sup>6</sup>Istituto Nazionale di Geofisica e Vulcanologia (INGV), OE, Catania, Italy

15 <sup>7</sup>Fondazione CIMA, Savona, Italy

*Correspondence to:* Camilo Naranjo ([camilo.naranjo@ingv.it](mailto:camilo.naranjo@ingv.it))

**Abstract.** Retrievals of volcanic clouds generated by eruptions are essential for effective emergency management. However, current methods have significant uncertainties due to the challenges of accurately measuring certain critical parameters through remote sensing. To address this, a new lightweight and low-cost multi-gas sensor instrument, called Volcanosonda, has been developed. It is designed to be deployed into volcanic clouds using sounding balloons, enabling in-situ measurements to enhance the characterization of these critical parameters. This work presents the measurements and cross-comparison results from an experiment conducted on Vulcano Island using the Volcanosonda alongside four well-established multi-gas sensor instruments. The results show an overall agreement between the measurements of SO<sub>2</sub> and CO<sub>2</sub> and the estimated CO<sub>2</sub>/SO<sub>2</sub> ratios.

## 1 Introduction

25 Volcanic eruptions inject large amounts of gases and particles into the atmosphere. These materials pose a significant threat to several aspects of human life: they can affect human health by causing respiratory issues (Stewart et al., 2021), impact the climate by increasing stratospheric aerosols that enhance Earth's albedo (Jenkins et al., 2023; Marshall et al., 2022), and disrupt aviation by causing engine failures, flight rerouting, and cancellations (Alexander, 2013; Prata and Rose, 2015).

Effective mitigation of these hazards requires accurate detection and quantification of volcanic cloud species (particles and gases 30 as CO<sub>2</sub>, SO<sub>2</sub>, H<sub>2</sub>S and HCl) and geometry (cloud altitude and thickness). To achieve these goals, several remote sensing instruments are currently used to monitor volcanic clouds (Pardini et al., 2024): ground-based systems include UltraViolet-UV (Burton et al., 2015; Campion et al., 2015; Tamburello et al., 2011), VISible-VIS (Simona Scollo et al., 2014), and Thermal InfraRed-TIR cameras (Guerrieri et al., 2025; Prata et al., 2024), lidars (Scollo et al., 2012), radars (Marzano et al., 2006, 2012;



Montopoli et al., 2014), and multi-gas sensor instruments (Aiuppa et al., 2005; Silvestri et al., 2023). Space-based observations 35 take advantage of the wide coverage provided by satellites, using UV and TIR sensors (for an exhaustive bibliography see Corradini et al., 2021), and microwave sensors (Marzano et al., 2018), spaceborne lidars (Burton et al., 2012), as well as the Global Navigate Satellite System (GNSS) observations (Cegla et al., 2022; Cigala et al., 2019).

Despite the availability of these instruments, their sensitivity and spatial resolution are limited, and all of them measure volcanic 40 cloud properties indirectly, leading to estimations with significant uncertainties (Corradini, 2008; Corradini et al., 2009; Pugnagh et al., 2013). These uncertainties arise from several critical parameters that are difficult to retrieve accurately, such as ash particle size distribution (PSD), ash composition, cloud thickness, and ash concentration. Moreover, the retrieval of gases as CO<sub>2</sub> is particularly challenging due to its significant presence in the atmosphere. Accurate information about these parameters can only be obtained through in-situ measurements, which is an approach that remains highly challenging.

Previous efforts have focused on in-situ measurements using multi-gas sensor instruments deployed on drones, Unmanned Aerial 45 Systems (UAS), and sounding balloons (Liu et al., 2020; Pieri et al., 2013; Silvestri et al., 2023; Stix et al., 2018; Vernier et al., 2020). However, the instruments employed in these measurements are often costly and weighty.

In order to improve the characterization of the cited critical volcanic clouds parameters, a new lightweight and low-cost multi-gas sensor system called “Volcanosonda” was developed within the framework of the VOlcanic pLume chAracterizatioN using sounDing ballOOns (VOLANDO) project (<https://progetti.ingv.it/it/volando>), a project funded by the European Union – Next 50 Generation EU within the Italian call “Progetti di Rilevante Interesse Nazionale” (PRIN). The Volcanosonda consists of a suite of sensors designed to measure the concentration and PSD of ash, as well as the concentrations of key volcanic gases (SO<sub>2</sub>, CO<sub>2</sub>), together with atmospheric parameters such as pressure, relative humidity, and temperature. The project aims to deploy the Volcanosonda into volcanic clouds using sounding balloons in free-flying and tethered configurations to perform in-situ measurements. These data are intended to improve and validate ash and SO<sub>2</sub> retrievals from both satellite and ground-based 55 observations (Pieri et al., 2013; Vernier et al., 2020).

To test the new Volcanosonda and its sensors, an experiment was conducted at the La Fossa crater on Vulcano Island (Aeolian Islands, Italy). In this case, measurements were taken at a fixed position and while the instrument was carried during walking, simultaneously with other four mature and well-established multi-gas instruments: HAPSITE SCOUT miniGAS, MiniGas NTX-PRO (Pieri et al., 2013; Silvestri et al., 2023; Stix et al., 2018; Vernier et al., 2020), Multi-Gas Labvulc and Multigas Drone PP 60 (Aiuppa et al., 2021, 2025; Burton et al., 2023; Liu et al., 2020) from University of Costa Rica, Istituto Nazionale di Geofisica e Vulcanologia - Osservatorio Nazionale Terremoti (INGV-ONT), the University of Palermo, and INGV-Osservatorio Etneo (OE) respectively. This experiment is part of a series of instrument tests conducted before deploying it in more intense events.

This work presents the results of the Vulcano Island field campaign, by analysing the Volcanosonda measurements, and making a cross-comparison between the different instruments. The data collected demonstrates the strong performance of the 65 Volcanosonda and its good agreement with the other instruments, indicating that the new system is ready for deployment into larger volcanic clouds.

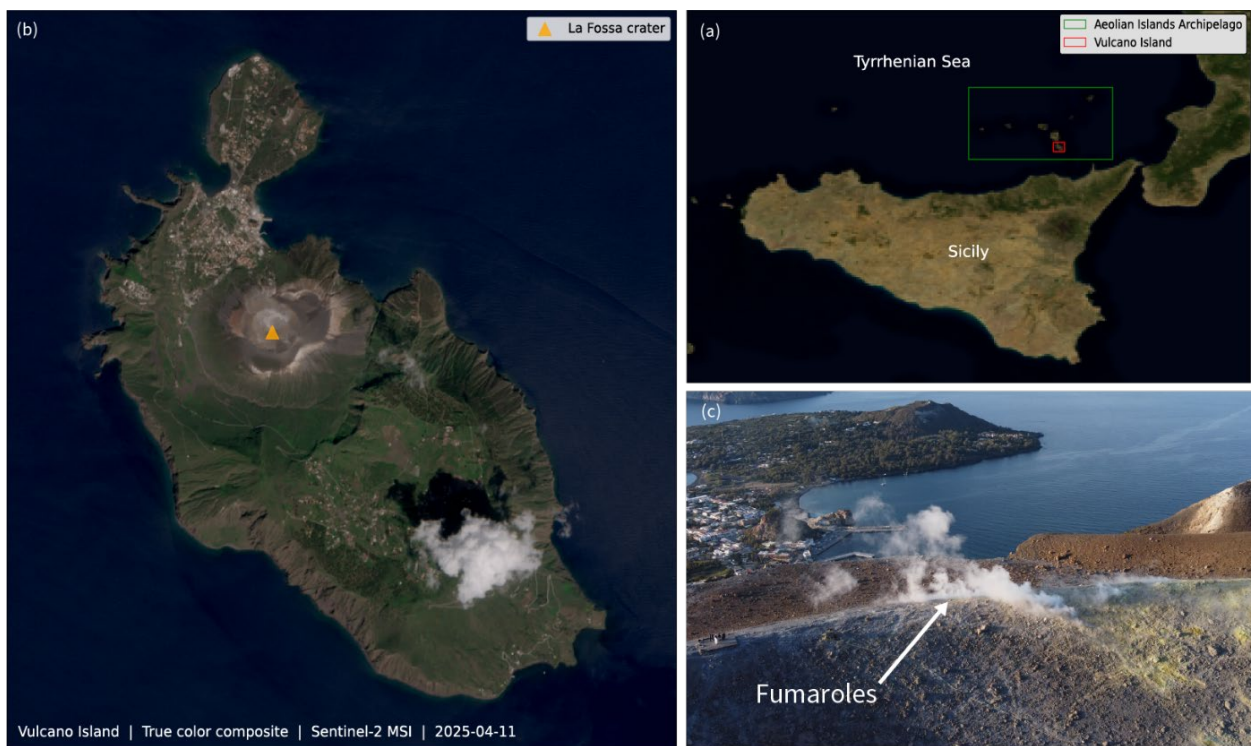
This paper is organized as follows: Section 2 introduces the selected test site. Section 3 describes the main features and



components of the Volcanosonda, and the other four instruments used to collect the measurements, as well as the setup of the experiment. Section 4 presents the data analysis, including the results and discussion of the cross-comparison among 70 instruments, with a focus on SO<sub>2</sub> and CO<sub>2</sub> measurements and the estimation of CO<sub>2</sub>/SO<sub>2</sub> ratios. Finally, Section 6 provides the conclusions.

## 2 Test site

The test site selected for the test measurements was the La Fossa crater on Vulcano Island (see Figure 1b). Vulcano is a stratovolcano located in the Aeolian Islands Archipelago, in the southern Tyrrhenian Sea (38.404°N, 14.962°E, see Figure 1a). 75 The volcano has a 3-km-wide crater and an elevation of 500 meters above sea level. The last major eruption at the La Fossa crater occurred between 1888 and 1890. Today, the predominant activity consists of fumarolic emissions, as shown in Figure 1c. This activity, along with low seismicity, makes the La Fossa crater a safe and ideal natural laboratory for conducting measurements to calibrate new instruments (Global Volcanism Program, 2025).



80 **Figure 1: Location map for the test site and fumarolic emissions. (a) Location of the Aeolian Islands Archipelago and Vulcano Island. (b) Vulcano Island, image captured by the Sentinel-2 satellite on April 11, 2025, one day after the field campaign. The orange triangle indicates the location of the La Fossa crater. (c) Northward-facing image taken by Jorge Andres Diaz using a drone on April 10, 2025, showing visible fumaroles along the rim of the La Fossa crater.**



## 85 3 Instruments and Experiment

This section presents details on the instruments employed in the measurements and describes the experiment carried out during the field campaign.

### 3.1 Instruments

A total of five instruments were deployed during the field campaign, contributed by collaborating institutions including INGV-

90 ONT, INGV-OE, the University of Pisa, the University of Palermo, and the University of Costa Rica. The following subsections provide a detailed description of the main technical characteristics of each instrument.

#### 3.1.1 Volcanosonda

The Volcanosonda instrument is a custom-designed multi-gas sensor package developed as part of the VOLANDO project, a joint effort between the Space Systems Laboratory of the University of Pisa and the Remote Sensing Group of INGV-ONT. The project 95 aims to develop a small, lightweight, and low-cost instrument, which can be deployed into volcanic plumes using sounding balloons to perform in-situ measurements.

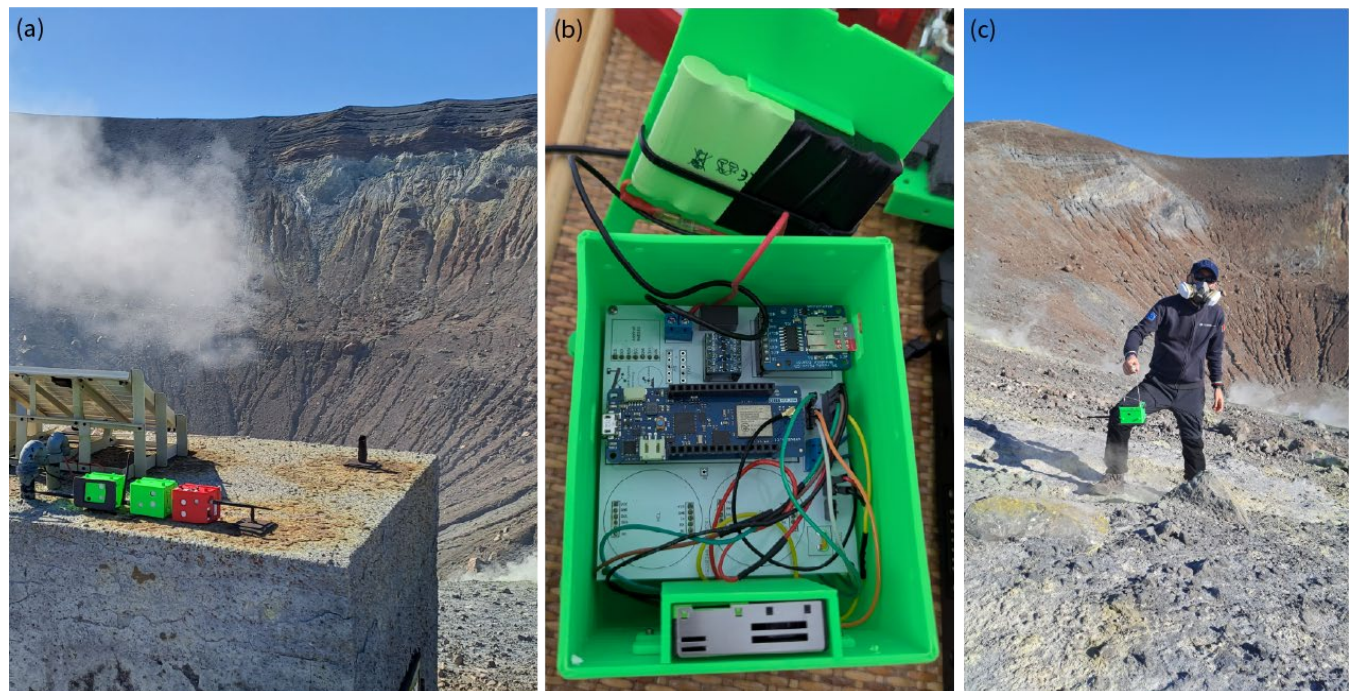


Figure 2: Photos of the volcanosonda. (a) The volcanosonda named 1D, 3D and 7D at the La Fossa crater. (b) Internal view 100 of the Volcanosonda instrument. (c) A Volcanosonda instrument being carried by an INGV researcher during the field campaign.



The Volcanosonda has dimensions of 14.0 cm × 11.7 cm × 9.5 cm and has a mass of 450 g. The instrument consists of a set of sensors integrated onto a circuit board, designed to measure ash concentration and key volcanic gases (SO<sub>2</sub> and CO<sub>2</sub>), as well as 105 atmospheric parameters including pressure, relative humidity, and temperature. The Volcanosonda acquires data at a frequency of 1 Hz, which is stored in onboard memory while simultaneously being transmitted to a ground station for real-time visualization via the Long Range (LoRa) protocol operating in the 868 MHz ISM band.

The SO<sub>2</sub> sensor is an electrochemical SO<sub>2</sub>-2000 developed by SemeaTech, the CO<sub>2</sub> sensor is a low power Non-Dispersive InfraRed (NDIR) CozIR-LP (5000 ppm) developed by Gas Sensing Solutions and the particles concentration is measured using an 110 optical particulate matter (PM) sensor SPS30 developed by Sensirion. The PM sensor provides the mass concentration for four particle size ranges: PM1, PM2.5, PM4, and PM10, which represent particles with diameters equal to or smaller than these values. The SO<sub>2</sub> sensor was calibrated at the Laboratory of the University of Palermo, and Table 1 provides a summary of the calibration measurements performed. Based on these data, the mean percentage error was determined to be approximately 18%. This value was subsequently used to calibrate all SO<sub>2</sub> measurements.

115 In contrast, for CO<sub>2</sub> measurements, only nominal pressure compensation was applied. According to the official documentation, the sensor is pre-calibrated at a reference pressure of 1013 mbar. When ambient pressure deviates from this value, the measurement varies by approximately 0.14% per mbar. The compensation was applied using Equation (1), where  $V_o$  represents the original value,  $V_c$  the compensated value and  $\Delta P$  represents the pressure difference between the reference value of 1013 mbar and the ambient pressure at which the measurements were taken. According to the manufacturer, the CO<sub>2</sub> sensor accuracy is 120 approximately ±30 ppm, with an additional ±3% of the measured value.

$$V_c = V_o + \left( \frac{\Delta P * 0.14}{100} \right) * V_o \quad (1)$$

125

**Table 1.** Summary of the calibration procedure and results for the SO<sub>2</sub> sensor.

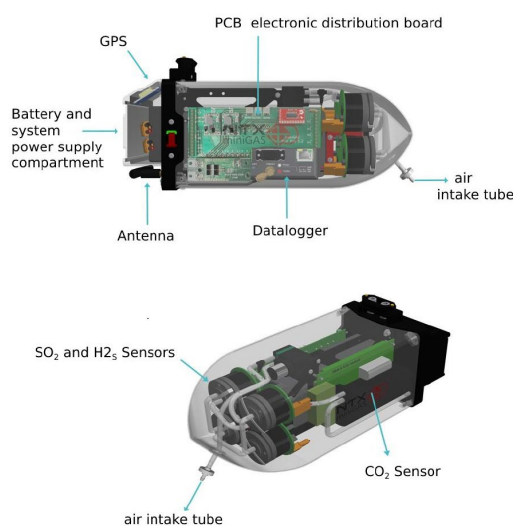
Test N°	Reference conditions		Measurements		Percent error [%]
	Value ± 4,0 [ppm]	Flux [L/min]	Value [ppm]	Bias [ppm]	
1	30.0	1.0	34.6	0.08	15.33
2	30.0	1.0	34.6	0.3	15.33
3	30.0	1.0	31.8	0.3	6.00
4	30.0	1.0	34.9	0.2	16.33
5	30.0	1.0	36.4	0.2	21.33
6	30.0	1.0	36.2	0.2	20.67
7	30.0	1.0	35.7	0.2	19.00
8	5.0	1.0	6.3	0.1	26.00
9	88.4	1.0	106.5	0.0	20.48



### 3.1.2 MiniGas NTX-PRO

130 The miniGAS NTX-PRO (see Figure 3) (Pieri et al., 2013; Silvestri et al., 2023; Stix et al., 2018; Vernier et al., 2020) is a portable multi-gas concentration measurement device weighing 1.5 kg, equipped with sensors for temperature, pressure, relative humidity, SO<sub>2</sub>, and H<sub>2</sub>S (electrochemical), along with a NDIR sensor for CO<sub>2</sub>. It also includes a Global Navigation Satellite System (GNSS) module, onboard data storage, and a mid-range Radio Frequency (RF) telemetry system with a connectivity range of up to 1.5 km, enabling real-time and remote in situ gas data acquisition.

135 With dimensions of 28 cm × 12 cm × 12 cm, the miniGAS NTX PRO is enclosed in an aerodynamic carbon fiber casing that protects the electronics from rain, vapours, ash, and wind. Its compact design makes it suitable for integration into small multirotor or fixed-wing drones, ground vehicles, or for handheld use in the field.



140 **Figure 3: MiniGAS PRO-NTX System.**

The PRO version incorporates a Campbell CR310 datalogger, which records measurements from a PP Systems SBA-5 OEM CO<sub>2</sub> infrared spectrometer (0–2000 ppm range) that also includes a solid-state water vapor pressure sensor (0–40 mbar range). Additionally, the datalogger captures signals from up to four City Technology (UK) electrochemical sensors: two for SO<sub>2</sub> 145 (EZT3ST/F; 0–200 ppm and 2TD2G-1A; 0–10 ppm), one for H<sub>2</sub>S (2TC4E-1AEZT3H; 0–50 ppm), and an optional H<sub>2</sub> sensor (T3HYT; 0–100 ppm).

Gas is sampled via an inlet positioned 1.2 meters away from the drone's core, a distance chosen to minimize disturbance from rotor-induced airflow and to ensure sampling of a more representative, undisturbed plume. The sample is drawn through the system using 1/4-inch Polytetrafluoroethylene (PTFE) tubing and a compact diaphragm pump operating at ~1.2 liters per minute. A 150 1.2 µm PTFE Teflon filter at the inlet prevents the entry of dust, particles, and fine droplets into the system.



Environmental parameters such as time, temperature, pressure, relative humidity, and GNSS location are recorded alongside gas concentration data. All data are transmitted and stored at a 1 Hz sampling rate, with real-time communication to a laptop via a Campbell Scientific RF-407 RPSMA radio transmitter operating in the 915–928 MHz frequency band.

The main features of the miniGAS PRO are listed in Table 2. The instrument has been deployed in several field campaigns

155 (Buongiorno et al., 2021, 2024; Diaz et al., 2015; de Moor et al., 2019; Pieri et al., 2013; Silvestri et al., 2015, 2016, 2021, 2023; Stix et al., 2018; Vernier et al., 2020).

**Table 2.** MiniGAS PRO-NTX Components.

Parameter	Description
Data logger	Campbell CR310
CO <sub>2</sub> Sensor	0–2000 ppm. PP System IR Spectrometer (SBA-5 OEM)
H <sub>2</sub> O Sensor	0–40 mbar range. Solid-state H <sub>2</sub> O partial pressure.
SO <sub>2</sub> Sensor (High)	0–200 ppm. Electrochemical City Technology. ECEZT3ST/F
SO <sub>2</sub> Sensor (Low)	0–10 ppm. Electrochemical City Technology 2TD2G-1A
H <sub>2</sub> S Sensor	0–50 ppm. Electrochemical City Technology 2TC4E-1AEZT3H;
Pump	1.2 lpm Thomas diaphragm pump
GNSS	Garmin 18x 5Hz GPS Navigator
Temperature	Thermocouple Type-K Glass Insulated
Radio	915–928 Mz . RF-407 RPSMA radio transmitter Campbell Scientific
Battery	LiPO 2200mAh. 11.1V. 5hr operation / Hot swappable

### 160 3.1.3 HAPSITE SCOUT miniGAS

The HAPSITE Scout (see Figure 4) (Pieri et al., 2013; Silvestri et al., 2023; Stix et al., 2018; Vernier et al., 2020) is a portable multi-gas analysis system similar to the miniGAS NTX-PRO version but developed in 2024 by INFICON, an international technology company specialized in the manufacture of instruments, sensor technologies, and process control monitoring for vacuum and gas analysis. It is designed for drone, UAV and robotic integration as well as hand portable and vehicle mobility surveys. It also incorporates a gas concentrator cartridge to collect a specific sample for further Gas Chromatography with Mass Spectrometry (GC-MS) analysis after collection. Figure 4 shows the Scout miniGAS attached to a drone for volcanic plume concentration mapping.

The Hapsite Scout uses the same sensors and geometry as the miniGAS NTX-PRO as described in Table 2 and Figure 3, with the addition of the gas sampling cartridge. The cartridge can also be substituted by a 1 L sample bag for sample collection and analysis.



**Figure 4: Hapsite Scout miniGAS System.**

### 3.1.4 Multi-Gas LabVulc

175 The Multi-GAS LabVulc (Aiuppa et al., 2021, 2025; Burton et al., 2023; Liu et al., 2020) is a custom-made multi-component gas analyzer system designed for the real-time measurement of volcanic gases, specifically CO<sub>2</sub>, SO<sub>2</sub>, H<sub>2</sub>S, H<sub>2</sub>, and H<sub>2</sub>O, at a frequency of 1 Hz. Compact, lightweight, and robust, the instrument is built for field use, especially during campaign-based volcanic gas surveys.

180 Weighing only 4 kg and housed in a rugged Peli case (33 × 29 × 15 cm), the system integrates commercially available components within a user-friendly and reliable setup. At the core of the instrument is a Campbell Scientific CR6 datalogger with integrated Wi-Fi, which manages data acquisition and communication. The system records CO<sub>2</sub> concentrations using a NDIR sensor (0–1% range) that also includes a pressure sensor, while additional electrochemical sensors (City Technology, UK) monitor SO<sub>2</sub>, H<sub>2</sub>S, and H<sub>2</sub>, each up to 200 ppm. Environmental parameters such as temperature, atmospheric pressure, relative humidity, and GNSS location are also recorded continuously.

185 Gas sampling is carried out using ¼ inch PTFE tubing and a compact diaphragm pump with a flow rate of approximately 1.2 liters per minute. A 1 µm PTFE Teflon filter at the inlet prevents dust, particles, and fine droplets from entering the system, ensuring sensor protection and data integrity.

190 The instrument is powered by a rechargeable Lithium polymer (LiPO) 4S or Lithium iron phosphate (LiFePO<sub>4</sub>) battery, allowing for fully portable operation. It supports two main operational modes: a portable mode, where acquisition is manually started and stopped by the operator during field surveys, and a permanent mode suitable for fix monitoring installations.

All acquired data are stored in Comma-Separated Values (CSV) format, with each recording session saved as a separate file. The system allows real-time data visualization on tablets or smartphones (iOS or Android) via a 2.4 GHz Wi-Fi connection using the Campbell Scientific LoggerLink App.



195 **Figure 5: Multi-GAS LabVulc.**

With its compact design, precise measurements, and ease of use, the Multi-GAS LabVulc is particularly suited for monitoring fumarolic emissions, plume and conducting volcanic gas studies in the field.

200 Sensor calibration is performed in the laboratory using a gas mixer to prepare mixtures of synthetic air and standard gases. The main features of the Multi-Gas LabVulc are listed in Table 3.

**Table 3.** Multi-GAS LabVulc Components.

Parameter	Description
Data logger	Campbell Scientific CR6 WiFi
CO <sub>2</sub> Sensor	0-1 %. Edinburgh Gascard NG infrared gas sensor
SO <sub>2</sub> Sensor	0-200 ppm. Electrochemical; City Technology. (Part n° TD2G-1A)
H <sub>2</sub> S Sensor	0-200 ppm. Electrochemical; City Technology. (Part n° TC4G-1A)
H <sub>2</sub> Sensor	0-200 ppm. Electrochemical; City Technology. (Part n° TE1G-1A)
Pump	1.2 lpm, Xavitech pump
GNSS	Adafruit Ultimate GPS Breakout
Rh/T	Humidity / temperature sensors KVM series
Pressure	Sensor on board Edinburgh Gascard
Transmission	WiFi 2.4 Giga – Tablet Android – LoggerLink Campbell App
Battery	LiPO 4S 5000 mAh 14.8V - with DC-DC stepdown



### 3.1.5 Multigas Drone PP

205 The Multi-GAS Drone PP (Aiuppa et al., 2021, 2025; Burton et al., 2023; Liu et al., 2020) is also a custom-made multi-component gas analyzer system designed for the real-time measurement of volcanic gases, specifically CO<sub>2</sub>, SO<sub>2</sub>, H<sub>2</sub>S, and H<sub>2</sub>O, at a frequency of 1 Hz similar to the Multi-Gas LabVulc. Compact, lightweight, and robust, the instrument is built for field use, especially during campaign-based volcanic gas surveys using drones.



210

**Figure 6: Multi-GAS Drone PP.**

Weighing only 875 g and housed in a light 3D printed case (13 × 9 × 16 cm), the system integrates commercially available components within a user-friendly and reliable setup. At the core of the instrument is a custom-made (INGV developed) Teodora 215 board datalogger, based on a Teensy microcontroller, with integrated Wi-Fi or radio link, which manages data acquisition and communication. The system records CO<sub>2</sub> concentrations using a PP System IR Spectrometer sensor, the additional electrochemical sensors (City Technology, UK) monitor SO<sub>2</sub> (200 ppm range) and H<sub>2</sub>S (up to 50 ppm). Environmental parameters such as temperature, atmospheric pressure, and GNSS location are also recorded continuously. Gas sampling and powering of the instrument are done similarly to the Multi-Gas LabVulc setup. The instrument supports drone mode operations but is also possible 220 to use in a portable mode, where acquisition is manually started and stopped by the operator during field surveys, and a permanent mode suitable for fix monitoring installations.

All acquired data are stored in CSV format and the system allows real-time data visualization on tablets or smartphones (iOS or Android) via a 2.4 GHz Wi-Fi connection or a radio link for drone mode, using a custom-made webserver app (developed at INGV-OE and Di3A-UniCT).

225



The Multi-GAS Drone PP is particularly suited for monitoring, plume and conducting volcanic gas studies in the field using fixed or rotary wing drones.

Sensor calibration is performed in the laboratory using a gas mixer to prepare mixtures of synthetic air and standard gases. The main features of the Multi-Gas Drone PP are listed in Table 4.

230

**Table 4.** Multi-GAS Drone PP Components.

Parameter	Description
Data logger	Teodora main board - Teensy 3.5 microcontroller
CO <sub>2</sub> Sensor	0–5000 ppm. PP System IR Spectrometer (SBA-5 OEM)
SO <sub>2</sub> Sensor	0–200 ppm. Electrochemical; City Technology. (Part n° TD2G-1A)
H <sub>2</sub> S Sensor	0–50 ppm. Electrochemical; City Technology. (Part n° TC4E-1A)
Pump	0.4 lpm Thomas diaphragm pump
GNSS	Adafruit Ultimate GPS Breakout
PTU	Pressure, Humidity, Temperature sensors: BlueDot BME280 Breakout Board
Transmission	RFD868 Long-range radio data modem operating in the 865-870MHz frequency band
UBEC	Matek UBEC DUO, 4A/5-12V & 4A/5V
Battery	LiPO 4S 1300 mAh 14.8V

### 3.2 Experiment

235 The objective of the experiment was to test the new Volcanosonda instruments and compare its measurements with other mature and well-established multi-gas instruments.

The experiment was carried out on the rim of the La Fossa crater on April 10, 2025, beginning at 10:26 local time (LT). At this time, all five instruments were positioned together in a fixed location (see Figure 7a), indicated by the yellow star in Figures 7c and 7d. The instruments collected measurements at this fixed point for approximately 25 minutes.

240 Afterward, the instruments were carried along the crater rim to acquire measurements while passing through the fumarolic area, as shown in Figure 7b and by the path indicated in Figure 7d. The first transect started at the yellow star and ended at the red point indicated in Figure 7c and 7d (~10 minutes). Finally, a second transect was conducted from the red point to the green point, also shown in Figure 7c and 7d (~14 minutes).

245



250



**Figure 7. Description of the experiment. (a) Instruments positioned together at a fixed location for data collection. (b) Instruments being carried along the rim of the La Fossa crater, passing through the fumarolic area. (c) West-facing photo showing the crater rim, visible fumaroles and key reference points: start (yellow), middle (red) and end (green). (d) Satellite view of the crater with the key reference points and the path followed during the experiment.**

255

#### 4 Data Analysis

This section presents the measurements acquired by the Volcanosonda sensors, along with the results of the cross-comparison

260 with the data collected by the other four instruments: HAPSITE SCOUT miniGAS, MiniGas NTX-PRO, Multi-Gas Labvulc, and Multigas Drone PP.



The experiment spanned approximately 50 minutes and was divided into three key time intervals for analysis. The first interval  
265 (T1) corresponds to the measurements collected at a fixed position at the start point and at the beginning of the first transect, before entering the fumarolic area. The second interval (T2) includes data gathered during the first transect, from the start point to the middle point. The third interval (T3) corresponds to the second transect, conducted from the middle point to the end point. Both the individual intervals and the complete time series are analysed to provide a comprehensive overview of the experiment.

#### 4.1 Volcanosonda measurements

270 All measurements collected by the Volcanosonda sensors are presented in Figure 8, which also indicates the three-time intervals (T1, T2 and T3). Figure 8a shows the data for temperature and relative humidity (RH). It is notable that RH remains relatively constant during T1, while significant variations occur during T2 and T3, corresponding to the periods when the instruments passed through the fumarolic area.

The data for SO<sub>2</sub> and pressure are shown in Figure 8b. It can be observed that SO<sub>2</sub> concentrations during T1 are low, with a mean  
275 value of 10 ppmv, while during T2 and T3, when the instrument was within the fumarolic area, the concentrations increase significantly, reaching maximum values of approximately 150 ppmv and a mean of 30.8 and 25.9 ppmv respectively. The pressure values show a descending trend from T2 and T3, which is consistent with the topography of the crater rim; as shown in Figure 7c, the middle point (marked in red) is slightly elevated compared to the start point.

In Figure 8c, CO<sub>2</sub> concentrations are shown alongside SO<sub>2</sub> concentrations for comparison. As explained in Section 3.1.1, the data  
280 presented have been corrected for pressure and calibrated for CO<sub>2</sub> and SO<sub>2</sub>, respectively. During T1, the mean CO<sub>2</sub> concentration was 548 ppmv. This value increased to 891.4 ppmv during T2 and 966.1 ppmv during T3, with maximum concentrations surpassing 2300 ppmv. Figure 8c also shows a good agreement between CO<sub>2</sub> and SO<sub>2</sub> concentrations, this is consistent with results obtained in previous works (Silvestri et al., 2023; Vernier et al., 2020). However, the CO<sub>2</sub> data show a noticeable delay relative to the SO<sub>2</sub> data, likely due to the response time of the CO<sub>2</sub> sensor. The response time is nominally around 30 seconds for  
285 the CO<sub>2</sub> sensor, but it is limited by diffusion through the membrane windows of the sensor, which becomes critical during rapid changes in concentration. This simultaneous analysis of CO<sub>2</sub> and SO<sub>2</sub> concentrations offers key information about volcanic gas composition and emission dynamics (Aiuppa et al., 2005).

Figure 8d presents the PM<sub>10</sub> concentrations alongside the SO<sub>2</sub> data and Figure 8e displays the full set of particulate matter (PM)  
290 concentrations, all of which exhibit similar behavior across the three-time intervals. Finally, Figures 8f–8i present the mean PM concentrations across four particle size ranges (0.0–1.0, 1.0–2.5, 2.5–4.0, and 4.0–10.0  $\mu\text{m}$ ). Concentrations are reported for each time interval (T1, T2, T3) and for the entire time series, showing a log-normal distribution.

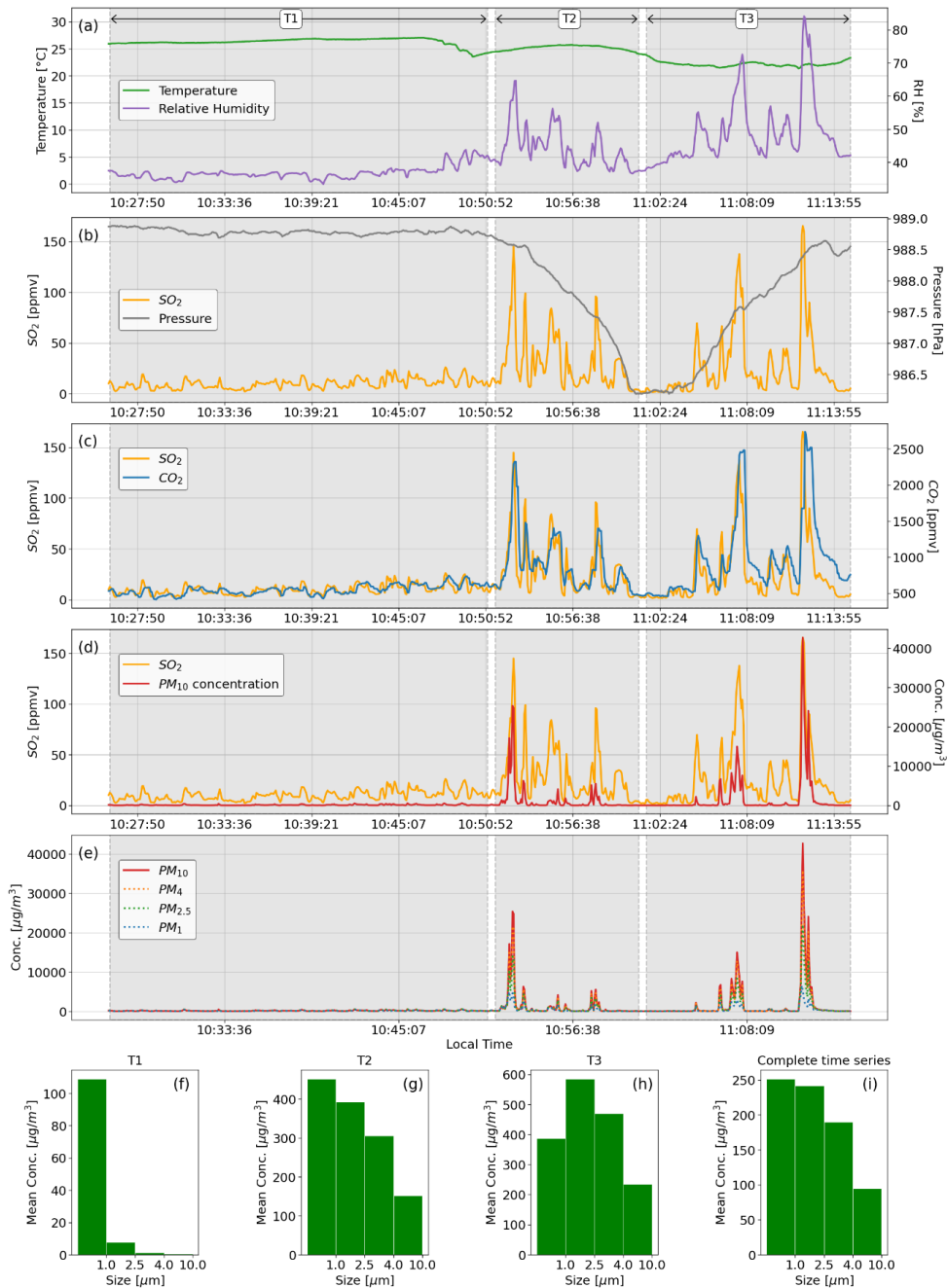


**Figure 8. Volcanosonda measurements. The three defined time intervals (T1, T2, and T3) are also specified in the figures.**

295 (a) Temperature and relative humidity measurements. (b)  $\text{SO}_2$  and pressure measurements. (c)  $\text{SO}_2$  and  $\text{CO}_2$  measurements. (d)  $\text{SO}_2$  and  $\text{PM}_{10}$  measurements. (e)  $\text{PM}$  concentration measurements for  $\text{PM}_1$ ,  $\text{PM}_{2.5}$ ,  $\text{PM}_4$ , and  $\text{PM}_{10}$ . (f)-(i) Mean  $\text{PM}$  concentrations for four particle size ranges (0.0–1.0, 1.0–2.5, 2.5–4.0, and 4.0–10.0  $\mu\text{m}$ ) reported for each time interval (T1, T2, T3) and the complete time series.



300 4.2 Comparative Analysis of Measurements

This subsection presents the cross-comparison of measurements collected by the five instruments. Figure 9a shows the CO<sub>2</sub> measurements across all instruments, while Figure 9b presents the corresponding SO<sub>2</sub> measurements. An appreciable agreement is observed among the measurement data collected across the instruments. Table 5 presents the mean CO<sub>2</sub> and SO<sub>2</sub> concentrations, which confirm the observed correspondence. That agreement is observed across instruments and across the different time

305 intervals.

When examining the Volcanosonda SO<sub>2</sub> data and comparing it with the other instruments, the agreement appears stronger than that observed for CO<sub>2</sub> measurements. The discrepancies observed in the CO<sub>2</sub> measurements may be attributed to the fact that the sampled gas was not identical across instruments, as the measurements were taken while carrying the instruments by hand and walking one after the other, as illustrated in Figure 7b. Additionally, with reference to the CO<sub>2</sub> sensor, these differences could be

310 influenced by the apparently slower response time and the accuracy of the CO<sub>2</sub> sensor.

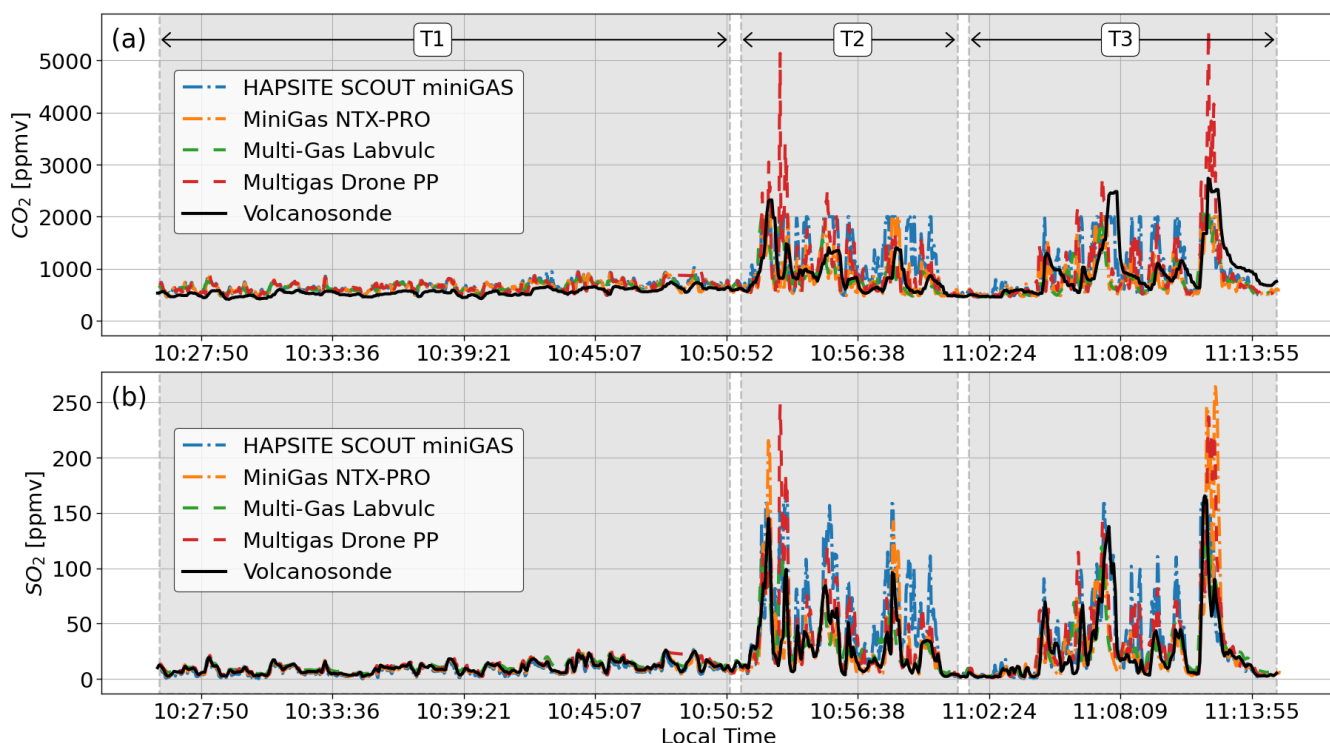


Figure 9. Measurement Comparison. (a) CO<sub>2</sub> data and (b) SO<sub>2</sub> data collected by the five instruments. The gray shaded areas indicate the defined time intervals.



**Table 5.** Mean CO<sub>2</sub> and SO<sub>2</sub> concentrations (in ppmv) obtained from each instrument across the defined time intervals (T1, T2, T3) and for the entire time series.

Variable	Time interval	Instruments				
		Volcanosonda	HAPSITE SCOUT miniGAS	MiniGas NTX-PRO	Multi-Gas Labvule	Multigas Drone PP
CO <sub>2</sub>	T1	548.0 ± 17	658.9 ± 7	646.9 ± 6	649.9 ± 13	649.4 ± 6
	T2	891.4 ± 28	1088.2 ± 11	823.4 ± 8	860.8 ± 17	1011.2 ± 10
	T3	966.1 ± 30	880.5 ± 9	754.2 ± 8	778.6 ± 16	927.9 ± 9
	Total time series	727.8 ± 23	787.9 ± 8	707.3 ± 7	724.9 ± 14	797.7 ± 8
SO <sub>2</sub>	T1	10.0 ± 2	8.2 ± 0.2	9.2 ± 0.2	11.8 ± 0.2	10.2 ± 0.2
	T2	30.8 ± 6	40.1 ± 0.8	26.7 ± 0.5	31.4 ± 0.6	39.5 ± 0.8
	T3	25.9 ± 5	24.6 ± 0.5	21.6 ± 0.4	25.0 ± 0.5	33.3 ± 0.7
	Total time series	18.2 ± 3	17.6 ± 0.4	15.8 ± 0.3	19.2 ± 0.4	22.5 ± 0.5

320

Subsequently, the CO<sub>2</sub> and SO<sub>2</sub> measurements from each instrument were time-shifted using cross-correlation analysis. This procedure was performed using the RatioCalc software (Tamburello, 2015) enabling alignment of the signal peaks, as demonstrated in Figure 10. This alignment is important for estimating the CO<sub>2</sub>/SO<sub>2</sub> ratio, which is discussed in the following subsection. The aligned CO<sub>2</sub> and SO<sub>2</sub> measurements for all five instruments are presented in Figures 10a–10e, illustrating the correlation between the CO<sub>2</sub> and SO<sub>2</sub> measurements across the instruments.

325

#### 4.2.1 CO<sub>2</sub>/SO<sub>2</sub> ratios

The previously aligned CO<sub>2</sub> and SO<sub>2</sub> data were used to estimate the instantaneous CO<sub>2</sub>/SO<sub>2</sub> ratios for each instrument, which are presented in Figure 11, where the comparison shows a generally good agreement across the instruments. The determination of the volcanic CO<sub>2</sub>/SO<sub>2</sub> ratios represent a key parameter in volcano monitoring because it is a marker based on the contrasting solubility properties of CO<sub>2</sub> and SO<sub>2</sub> (Aiuppa et al., 2025; Tamburello, 2015).

330 Additionally, the CO<sub>2</sub>/SO<sub>2</sub> ratios for each instrument during each time interval, were estimated using the RatioCalc software (Tamburello, 2015). For this estimation the saturated values, especially those present in the HAPSITE SCOUT miniGAS and MiniGas NTX-PRO data (see Figure 10b and 10c) were not considered in the analysis.

335

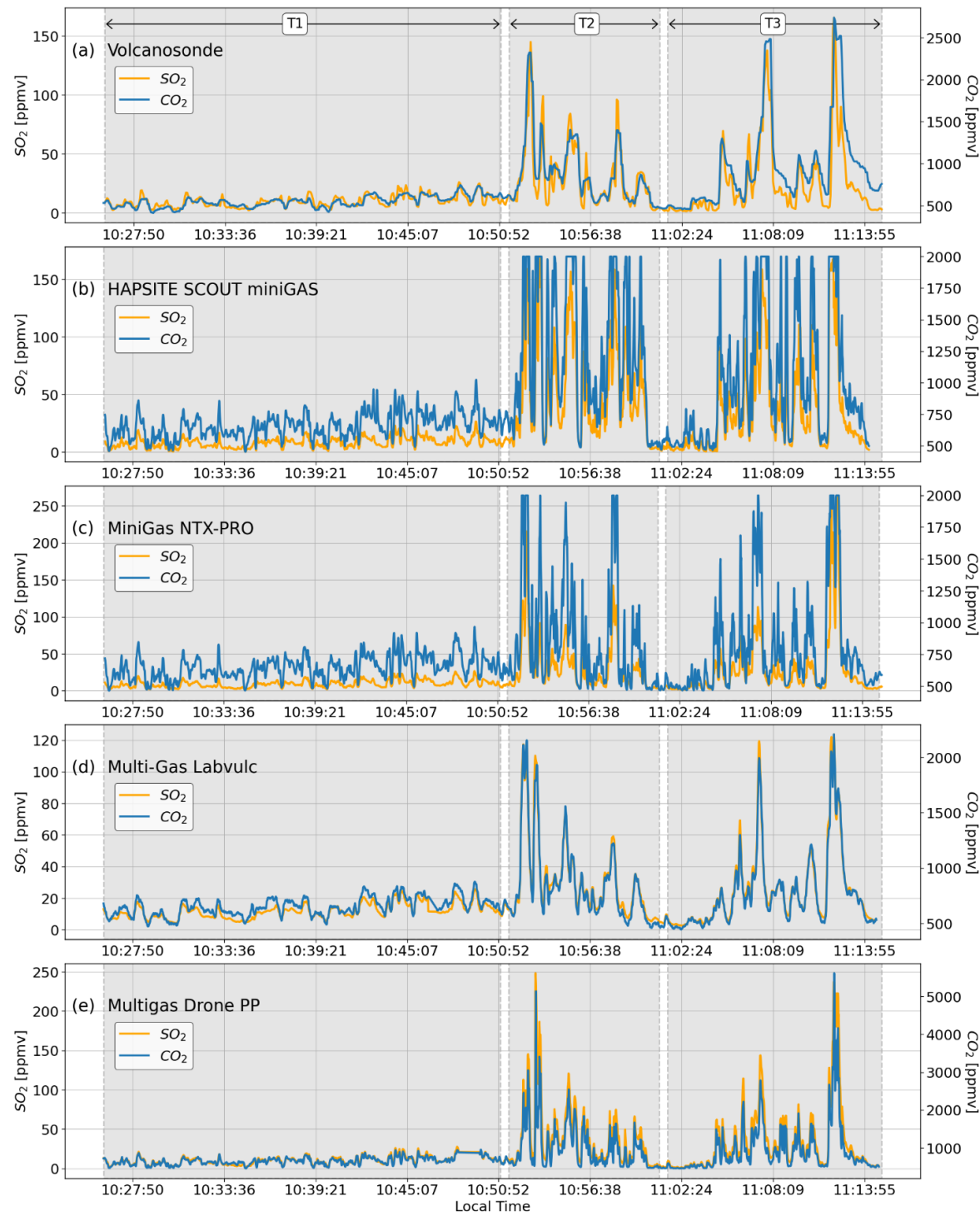
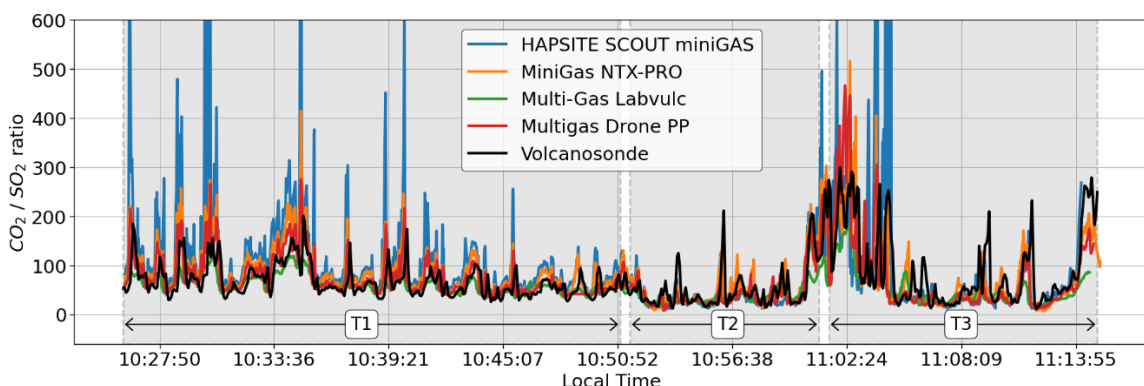


**Figure 10. Aligned  $\text{CO}_2$  and  $\text{SO}_2$  measurements for: (a) Volcanosonda, (b) HAPSITE SCOUT miniGAS, (c) MiniGas NTX-PRO, (d) Multi-Gas Labvulc and (e) Multigas Drone PP.**



The CO<sub>2</sub>/SO<sub>2</sub> ratios correspond to the slope values obtained from a linear regression model applied to the measurement data 340 (Aiuppa et al., 2005; Stix et al., 2018; Tamburello, 2015). The resulting ratio values are summarized in Table 6, while the corresponding model fits are illustrated in Figure 12, which also includes the coefficients of determination (R<sup>2</sup>) for each case. The coefficients R<sup>2</sup> quantify how strong is the correlation between CO<sub>2</sub> and SO<sub>2</sub> measurements for each instrument across the defined time intervals (T1, T2, T3) and for the complete time series.

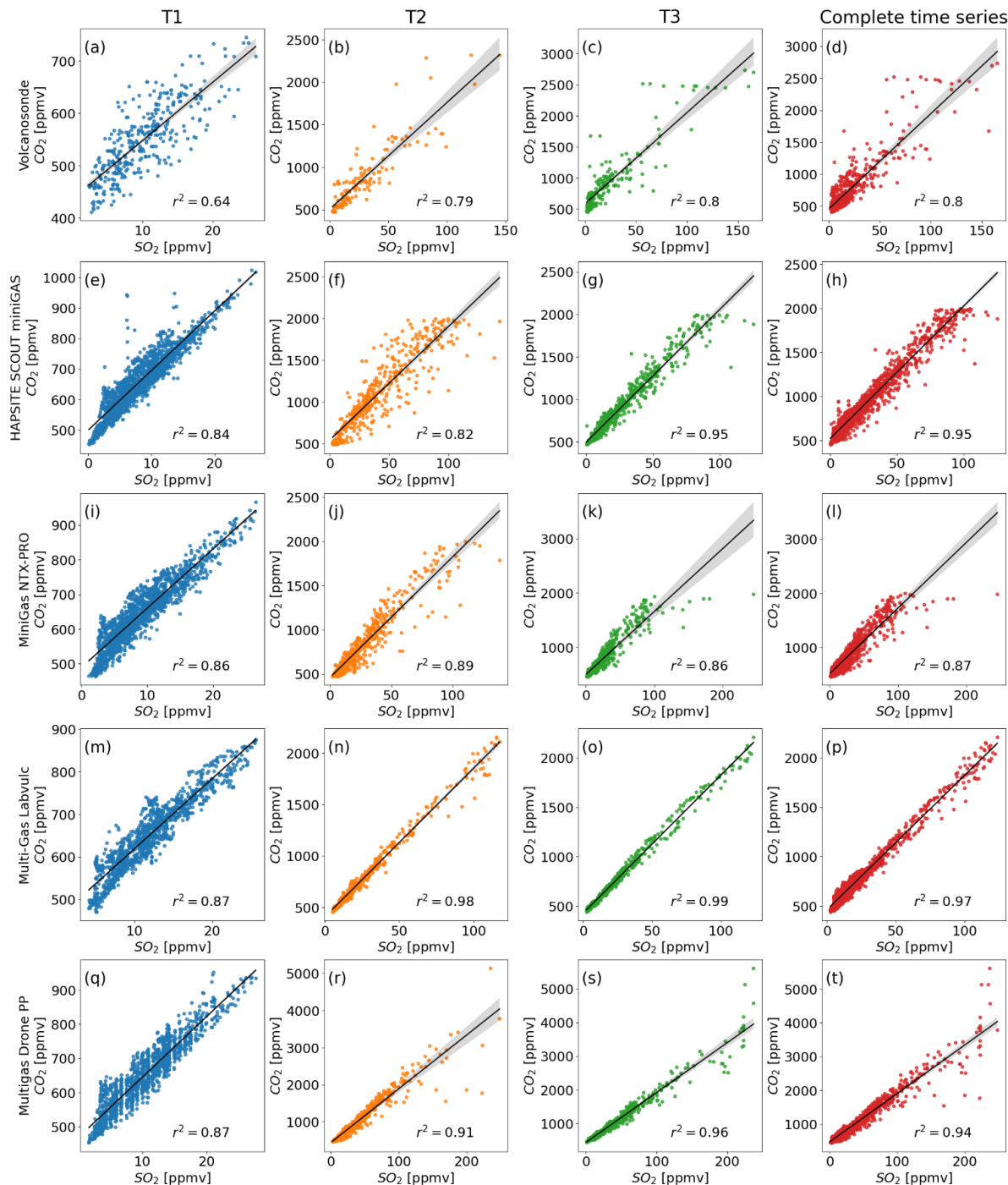


345 **Figure 11. Instantaneous CO<sub>2</sub>/SO<sub>2</sub> ratio comparison.**

**Table 6.** Summary of CO<sub>2</sub>/SO<sub>2</sub> ratios for each instrument.

Time interval	Instruments				
	Volcanosonda	HAPSITE SCOUT miniGAS	MiniGas NTX-PRO	Multi-Gas Labvulc	Multigas Drone PP
T1	11.12	19.52	17.11	16.47	17.75
T2	12.56	13.62	13.67	14.48	14.52
T3	14.64	15.62	11.54	13.97	14.87
Total time series	14.89	15.05	12.10	13.61	14.35

350 In general, the CO<sub>2</sub>/SO<sub>2</sub> ratios obtained for the Volcanosonda are in good agreement with the ratios obtained for the other four instruments, as we can see in Table 6. It should be noted, however, that a trend is observed across the T1, T2, and T3 intervals for the four other instruments, in which the CO<sub>2</sub>/SO<sub>2</sub> ratios during T1 are slightly higher than those during T2 and T3. This trend is reasonable, as during T2 and T3 the instruments went into the fumarolic area, where SO<sub>2</sub> concentrations increased, leading to lower CO<sub>2</sub>/SO<sub>2</sub> ratios (Aiuppa et al., 2005; Vernier et al., 2020). Whereas during T1, the Volcanosonda reported its lowest 355 CO<sub>2</sub>/SO<sub>2</sub> ratio, with a value of 11.12. Another notable difference is observed in Figure 12a, where the linear regression for the Volcanosonda during T1 shows an R<sup>2</sup> value of 0.64, the lowest among all the analyses performed across the instruments. These discrepancies may likely be attributed to the accuracy and time response of the CO<sub>2</sub> sensor, as mentioned previously in the sections 4.1 and 4.2.



360 **Figure 12. Linear regression comparison between CO<sub>2</sub> and SO<sub>2</sub> measurements. The columns represent the time intervals (T1, T2, and T3), while the rows correspond to each instrument. The coefficients of determination (R<sup>2</sup>) are displayed for each case.**



#### 4 Conclusions

This work presents the experiment results from a new lightweight and low-cost multi-gas sensor instrument called 365 “Volcanosonda”, which was developed to fly into volcanic clouds to perform in-situ measurements. The principal objective of this new multi-gas sensor is to enhance the characterization of several volcanic cloud parameters that are difficult to retrieve accurately, such as ash PSD, particles and gases concentration and cloud geometry (altitude and thickness). With all this information the idea is then to improve and validate ash and SO<sub>2</sub> retrievals from both satellite and ground-based observations.

Other authors have been carried out in-situ measurements using multi-gas sensor instruments (Pieri et al., 2013; Silvestri et al., 370 2023; Stix et al., 2018; Vernier et al., 2020), but the novel of the Volcanosonda is the lightweight and low-cost. Therefore, a cross-comparison experiment was performed using four other mature and well-established multi-gas instruments. Compared to the other multi-gas instruments the Volcanosonda is 50% to 90% lighter.

The results showed that the Volcanosonda’s measurements of CO<sub>2</sub> and SO<sub>2</sub> concentrations agreed with those of the other instruments. This agreement is evident from the CO<sub>2</sub>/SO<sub>2</sub> ratio values and the R<sup>2</sup> values presented in Table 6 and Figure 12, 375 respectively. The R<sup>2</sup> value for the Volcanosonda is 0.64 for T1 and approximately 0.8 for the other time slots. Although these R<sup>2</sup> values are slightly lower than those of the other instruments, they still indicate a strong correlation between the CO<sub>2</sub> and SO<sub>2</sub> measurements.

We identify some differences, especially with the CO<sub>2</sub> sensor measurements. We think the differences are related to the time 380 response of the sensor, which becomes critical during rapid changes in concentration. Future work should focus on characterizing the CO<sub>2</sub> sensor time response for this application.

However, the other sensors like the SO<sub>2</sub> and the optical particulate matter have an optimal performance. Our results are encouraging and our new Volcanosonda instrument is ready for deployment into larger volcanic clouds and helping to enhance the retrieval of volcanic clouds.

#### Data availability

385 All data analysed in this study were obtained from the five instruments described above and will be made available upon reasonable request.

#### Author contributions

Writing (original draft preparation): CN and SC. Conceptualization: CN and SC. Data curation: CN, MB, EC, JAD, AF, GG. Formal Analysis: CN, SC, RB, AF, MG, LG, IM, LM, DS. Funding acquisition: SC, RB, SM. Investigation (Data collection): CN, 390 SC, MB, MFB, JAD, AF, GG, MS, AV. Methodology: CN, SC, GG. Project administration: SC, RB, SM. Software: CN and AF. Supervision: SC, RB, SM. Visualization: CN. Writing (review and editing): All authors.



## Competing interests Data availability

Authors declare no competing interests related to this work.

## Disclaimer

395 Copernicus Publications remains neutral with regard to jurisdictional claims made in the text, published maps, institutional affiliations, or any other geographical representation in this paper. While Copernicus Publications makes every effort to include appropriate place names, the final responsibility lies with the authors. Views expressed in the text are those of the authors and do not necessarily reflect the views of the publisher.

## Acknowledgements

400 This work contains modified Copernicus Sentinel-2 data [2025] processed by the authors.

## Financial support

This research was supported by the VOLANDO (VOLcanic pLume chAracterization using sounNDing balloOns) project funded by European Union - Next Generation EU, Missione 4 Componente 1 CUP D53D23004910006.

## References

405 Aiuppa, A., Federico, C., Giudice, G., and Gurrieri, S.: Chemical mapping of a fumarolic field: La Fossa Crater, Vulcano Island (Aeolian Islands, Italy), *Geophys. Res. Lett.*, 32, 1–4, <https://doi.org/10.1029/2005GL023207>, 2005.

Aiuppa, A., Bitetto, M., Donne, D. D., la Monica, F. P., Tamburello, G., Coppola, D., Schiava, M. Della, Innocenti, L., Lacanna, G., Laiolo, M., Massimetti, F., Pistoletti, M., Silengo, M. C., and Ripepe, M.: Volcanic CO<sub>2</sub> tracks the incubation period of basaltic paroxysms, *Sci. Adv.*, 7, 191–208, <https://doi.org/10.1126/SCIADV.ABH0191>, 2021.

410 Aiuppa, A., Bitetto, M., Curcio, L., Delle Donne, D., Lages, J., Lo Bue Trisciuozzi, G., Tamburello, G., Vitale, A., Cannavò, F., Coltellini, M., Coppola, D., Innocenti, L., Insinga, L., Lacanna, G., Laiolo, M., Massimetti, F., Pistoletti, M., Privitera, E., Ripepe, M., Voloschina, M., and Cilluffo, G.: Volcanic gas changes prior to Stromboli's major explosions are statistically significant, *Journal of Volcanology and Geothermal Research*, 462, 108325, <https://doi.org/10.1016/J.JVOLGEORES.2025.108325>, 2025.

Alexander, D.: Volcanic ash in the atmosphere and risks for civil aviation: A study in European crisis management, *International Journal of Disaster Risk Science*, 4, 9–19, <https://doi.org/10.1007/S13753-013-0003-0>/METRICS, 2013.

415 Buongiorno, M. F., Silvestri, M., Romaniello, V., Marotta, E., Caputo, T., Musacchio, M., Rabuffi, F., Sessa, E. B., Diaz, J. A., Avvisati, G., and Belviso, P.: Space Missions, Drones and Cameras in Situ for Thermal Analysis and Gas Retrieval in Volcanic



Areas, in: 2021 IEEE International Geoscience and Remote Sensing Symposium IGARSS, 984–987, <https://doi.org/10.1109/IGARSS47720.2021.9555167>, 2021.

420 Buongiorno, M. F., Rabuffi, F., Silvestri, M., Marotta, E., Belviso, P., Inguaggiato, S., Vita, F., Pisciotta, F. A., Hook, S., Rivera, G., Corrales, E., Diaz, J. A., and Venafra, S.: Preliminary Results of the Cal/Val Activity over Eolian Island During the HyTES 2023 European Airbone Campaign., in: IGARSS 2024 - 2024 IEEE International Geoscience and Remote Sensing Symposium, 3572–3575, <https://doi.org/10.1109/IGARSS53475.2024.10642065>, 2024.

Burton, M., Aiuppa, A., Allard, P., Asensio-Ramos, M., Cofrades, A. P., La Spina, A., Nicholson, E. J., Zanon, V., Barrancos, J., 425 Bitetto, M., Hartley, M., Romero, J. E., Waters, E., Stewart, A., Hernández, P. A., Lages, J. P., Padrón, E., Wood, K., Esse, B., Hayer, C., Cyrzan, K., Rose-Koga, E. F., Schiavi, F., D'Auria, L., and Pérez, N. M.: Exceptional eruptive CO<sub>2</sub> emissions from intra-plate alkaline magmatism in the Canary volcanic archipelago, *Commun. Earth Environ.*, 4, 1–10, <https://doi.org/10.1038/S43247-023-01103-X>;SUBJMETA, 2023.

Burton, M. R., Prata, F., and Platt, U.: Volcanological applications of SO<sub>2</sub> cameras, *Journal of Volcanology and Geothermal Research*, 300, 2–6, <https://doi.org/10.1016/j.jvolgeores.2014.09.008>, 2015.

Burton, S. P., Ferrare, R. A., Hostetler, C. A., Hair, J. W., Rogers, R. R., Oblad, M. D., Butler, C. F., Cook, A. L., Harper, D. B., and Froyd, K. D.: Aerosol classification using airborne High Spectral Resolution Lidar measurements – methodology and examples, *Atmos. Meas. Tech.*, 5, 73–98, <https://doi.org/10.5194/amt-5-73-2012>, 2012.

Campion, R., Delgado-Granados, H., and Mori, T.: Image-based correction of the light dilution effect for SO<sub>2</sub> camera 435 measurements, *Journal of Volcanology and Geothermal Research*, 300, 48–57, <https://doi.org/10.1016/j.jvolgeores.2015.01.004>, 2015.

Cegla, A., Rohm, W., Lasota, E., and Biondi, R.: Detecting volcanic plume signatures on GNSS signal, Based on the 2014 Sakurajima Eruption, *Advances in Space Research*, 69, 292–307, <https://doi.org/10.1016/J.ASR.2021.08.034>, 2022.

Cigala, V., Biondi, R., Prata, A. J., Steiner, A. K., Kirchengast, G., and Brenot, H.: GNSS Radio Occultation Advances the 440 Monitoring of Volcanic Clouds: The Case of the 2008 Kasatochi Eruption, *Remote Sensing* 2019, Vol. 11, Page 2199, 11, 2199, <https://doi.org/10.3390/RS11192199>, 2019.

Corradini, S.: Mt. Etna tropospheric ash retrieval and sensitivity analysis using moderate resolution imaging spectroradiometer measurements, *J. Appl. Remote Sens.*, 2, 023550, <https://doi.org/10.1117/1.3046674>, 2008.

Corradini, S., Merucci, L., and Prata, A. J.: Retrieval of SO<sub>2</sub> from thermal infrared satellite measurements: Correction procedures 445 for the effects of volcanic ash, *Atmos. Meas. Tech.*, 2, 177–191, <https://doi.org/10.5194/AMT-2-177-2009>, 2009.

Corradini, S., Guerrieri, L., Brenot, H., Clarisse, L., Merucci, L., Pardini, F., Prata, A. J., Realmuto, V. J., Stelitano, D., and Theys, N.: Tropospheric Volcanic SO<sub>2</sub> Mass and Flux Retrievals from Satellite. The Etna December 2018 Eruption, *Remote Sens. (Basel)*, 13, 2225, <https://doi.org/10.3390/rs13112225>, 2021.

Diaz, J. A., Pieri, D., Wright, K., Sorensen, P., Kline-Shoder, R., Arkin, C. R., Fladeland, M., Bland, G., Buongiorno, M. F., 450 Ramirez, C., Corrales, E., Alan, A., Alegria, O., Diaz, D., and Linick, J.: Unmanned Aerial Mass Spectrometer Systems for In-Situ Volcanic Plume Analysis, *J. Am. Soc. Mass Spectrom.*, 26, 292–304, <https://doi.org/10.1007/s13361-014-1058-x>, 2015.



Global Volcanism Program: Volcano (211050) in [Database] Volcanoes of the World, Distributed by Smithsonian Institution, compiled by Venzke, E. , Global Volcanism Program, <https://doi.org/10.5479/SI.GVP.VOTW5-2024.5.2>, 2025.

455 Guerrieri, L., Corradini, S., Merucci, L., Stelitano, D., Prata, F., Lambertucci, L., Naranjo, C., and Biondi, R.: A Novel Simplified Ground-Based TIR System for Volcanic Plume Geometry, SO<sub>2</sub> Columnar Abundance, and Flux Retrievals, <https://doi.org/10.5194/EGUSPHERE-2025-63>, 2025.

Jenkins, S., Smith, C., Allen, M., and Grainger, R.: Tonga eruption increases chance of temporary surface temperature anomaly above 1.5 °C, Nat. Clim. Chang., 13, 127–129, <https://doi.org/10.1038/S41558-022-01568-2>;SUBJMETA=106,1108,2786,674,694,704;KWRD=ATTRIBUTION,CLIMATE+AND+EARTH+SYSTEM+MODELLING,PR

460 OJECTION+AND+PREDICTION, 2023.

Liu, E. J., Aiuppa, A., Alan, A., Arellano, S., Bitetto, M., Bobrowski, N., Carn, S., Clarke, R., Corrales, E., de Moor, J. M., Diaz, J. A., Edmonds, M., Fischer, T. P., Freer, J., Fricke, G. M., Galle, B., Gerdes, G., Giudice, G., Gutmann, A., Hayer, C., Itikarai, I., Jones, J., Mason, E., McCormick Kilbride, B. T., Mulina, K., Nowicki, S., Rahilly, K., Richardson, T., Rüdiger, J., Schipper, C. I., Watson, I. M., and Wood, K.: Aerial strategies advance volcanic gas measurements at inaccessible, strongly degassing volcanoes, [Sci. Adv.](https://doi.org/10.1126/sciadv.abb9103), 6, <https://doi.org/10.1126/sciadv.abb9103>, 2020.

Marshall, L. R., Maters, E. C., Schmidt, A., Timmreck, C., Robock, A., and Toohey, M.: Volcanic effects on climate: recent advances and future avenues, *Bulletin of Volcanology* 2022 84:5, 84, 1–14, <https://doi.org/10.1007/S00445-022-01559-3>, 2022.

Marzano, F. S., Barbieri, S., Vulpiani, G., and Rose, W. I.: Volcanic Ash Cloud Retrieval by Ground-Based Microwave Weather Radar, *IEEE Transactions on Geoscience and Remote Sensing*, 44, 3235–3246, <https://doi.org/10.1109/TGRS.2006.879116>, 2006.

470 Marzano, F. S., Picciotti, E., Vulpiani, G., and Montopoli, M.: Synthetic Signatures of Volcanic Ash Cloud Particles From X-Band Dual-Polarization Radar, *IEEE Transactions on Geoscience and Remote Sensing*, 50, 193–211, <https://doi.org/10.1109/TGRS.2011.2159225>, 2012.

Marzano, F. S., Corradini, S., Mereu, L., Kylling, A., Montopoli, M., Cimini, D., Merucci, L., and Stelitano, D.: Multisatellite Multisensor Observations of a Sub-Plinian Volcanic Eruption: The 2015 Calbuco Explosive Event in Chile, *IEEE Transactions on Geoscience and Remote Sensing*, 56, 2597–2612, <https://doi.org/10.1109/TGRS.2017.2769003>, 2018.

Montopoli, M., Vulpiani, G., Cimini, D., Picciotti, E., and Marzano, F. S.: Interpretation of observed microwave signatures from ground dual polarization radar and space multi-frequency radiometer for the 2011 Grímsvötn volcanic eruption, *Atmos. Meas. Tech.*, 7, 537–552, <https://doi.org/10.5194/amt-7-537-2014>, 2014.

de Moor, J. M., Stix, J., Avard, G., Muller, C., Corrales, E., Diaz, J. A., Alan, A., Brenes, J., Pacheco, J., Aiuppa, A., and Fischer, T. P.: Insights on Hydrothermal-Magmatic Interactions and Eruptive Processes at Poás Volcano (Costa Rica) From High-Frequency Gas Monitoring and Drone Measurements, *Geophys. Res. Lett.*, 46, 1293–1302, <https://doi.org/10.1029/2018GL080301>, 2019.

Pardini, F., Barsotti, S., Bonadonna, C., Vitturi, M. de' M., Folch, A., Mastin, L., Osores, S., and Prata, A. T.: Dynamics, Monitoring, and Forecasting of Tephra in the Atmosphere, *Reviews of Geophysics*, 62, e2023RG000808, <https://doi.org/10.1029/2023RG000808>, 2024.



Pieri, D., Diaz, J. A., Bland, G., Fladeland, M., Madrigal, Y., Corrales, E., Alegria, O., Alan, A., Realmuto, V., Miles, T., and Abtahi, A.: In situ observations and sampling of volcanic emissions with NASA and UCR unmanned aircraft, including a case study at turrialba volcano, Costa rica, Geol. Soc. Spec. Publ., 380, 321–352, <https://doi.org/10.1144/SP380.13>; CTYPE:STRING:JOURNAL, 2013.

490 Prata, F. and Rose, B.: Volcanic Ash Hazards to Aviation, The Encyclopedia of Volcanoes, 911–934, <https://doi.org/10.1016/B978-0-12-385938-9.00052-3>, 2015.

Prata, F., Corradini, S., Biondi, R., Guerrieri, L., Merucci, L., Prata, A., and Stelitano, D.: Applications of Ground-Based Infrared Cameras for Remote Sensing of Volcanic Plumes, Geosciences 2024, Vol. 14, Page 82, 14, 82, <https://doi.org/10.3390/GEOSCIENCES14030082>, 2024.

495 Pugnaghi, S., Guerrieri, L., Corradini, S., Merucci, L., and Arvani, B.: A new simplified approach for simultaneous retrieval of SO<sub>2</sub> and ash content of tropospheric volcanic clouds: an application to the Mt Etna volcano, Atmos. Meas. Tech., 6, 1315–1327, <https://doi.org/10.5194/amt-6-1315-2013>, 2013.

Scollo, S., Boselli, A., Coltelli, M., Leto, G., Pisani, G., Spinelli, N., and Wang, X.: Monitoring Etna volcanic plumes using a scanning LiDAR, Bull. Volcanol., 74, 2383–2395, <https://doi.org/10.1007/s00445-012-0669-y>, 2012.

500 Silvestri, M., Diaz, J. A., Marotta, E., Musacchio, M., Buongiorno, M. F., Sansivero, F., Cardellini, C., Pieri, D., Amici, S., Bagnato, E., Beddini, G., Belviso, P., Carandente, A., Colini, L., Doumaz, F., Peluso, R., and Spinetti, C.: Use of Multiple in situ and remote sensing instruments and techniques at Solfatara field campaign for measurements of CO<sub>2</sub>, H<sub>2</sub>S and SO<sub>2</sub> emissions: Special demonstration on unmanned aerial systems., Quaderni di Geofisica, 129, 2015.

Silvestri, M., Diaz, J. A., Vita, F., Musacchio, M., Puchalla, J., Falcone, S., Buongiorno, M. F., Doumaz, F., and Wright, K.:

505 Improved instruments for volcanic plume observation for monitoring purpose: Solfatara and Vulcano island preliminary results, Rapporti Tecnici INGV, 349, 2016.

Silvestri, M., Diaz, J. A., Marotta, E., Dalla Via, G., Bellucci Sessa, E., Caputo, T., Buongiorno, M. F., Sansivero, F., Musacchio, M., Belviso, P., Carandente, A., Peluso, R., Nave, R., Vilardo, G., Doumaz, F., and Corrales, E.: The 2016 field campaign of La Solfatara volcano: monitoring methods and instruments for volcanic surveillance, Rapporti Tecnici INGV, 380, <https://doi.org/https://doi.org/10.13127/rpt/380>, 2021.

510 Silvestri, M., Diaz, J. A., Rabuffi, F., Romaniello, V., Musacchio, M., Corrales, E., Fox, J., Marotta, E., Belviso, P., Avino, R., Avvisati, G., and Buongiorno, M. F.: MultiGAS Detection from Airborne Platforms on Italian Volcanic and Geothermal Areas, Remote Sensing 2023, Vol. 15, Page 2390, 15, 2390, <https://doi.org/10.3390/RS15092390>, 2023.

Simona Scollo, Michele Prestifilippo, Emilio Pecora, Stefano Corradini, Luca Merucci, Gaetano Spata, and Mauro Coltelli:

515 Eruption column height estimation of the 2011-2013 Etna lava fountains, Annals of Geophysics, 57, <https://doi.org/10.4401/ag-6396>, 2014.

Stewart, C., Damby, D. E., Horwell, C. J., Elias, T., Ilyinskaya, E., Tomašek, I., Longo, B. M., Schmidt, A., Carlsen, H. K., Mason, E., Baxter, P. J., Cronin, S., and Witham, C.: Volcanic air pollution and human health: recent advances and future directions, Bulletin of Volcanology 2021 84:1, 84, 1–25, <https://doi.org/10.1007/S00445-021-01513-9>, 2021.



520 Stix, J., de Moor, J. M., Rüdiger, J., Alan, A., Corrales, E., D'Arcy, F., Diaz, J. A., and Liotta, M.: Using Drones and Miniaturized Instrumentation to Study Degassing at Turrialba and Masaya Volcanoes, Central America, *J. Geophys. Res. Solid Earth*, 123, 6501–6520, <https://doi.org/10.1029/2018JB015655>, 2018.

Tamburello, G.: Ratiocalc: Software for processing data from multicomponent volcanic gas analyzers, *Comput. Geosci.*, 82, 63–67, <https://doi.org/10.1016/J.CAGEO.2015.05.004>, 2015.

525 Tamburello, G., Kantzas, E. P., McGonigle, A. J. S., Aiuppa, A., and Giudice, G.: UV camera measurements of fumarole field degassing (La Fossa crater, Vulcano Island), *Journal of Volcanology and Geothermal Research*, 199, 47–52, <https://doi.org/10.1016/j.jvolgeores.2010.10.004>, 2011.

Vernier, J. P., Kalnajs, L., Diaz, J. A., Reese, T., Corrales, E., Alan, A., Vernier, H., Holland, L., Patel, A., Rastogi, N., Wienhold, F., Carn, S., Krotkov, N., and Murray, J.: VolKila: Volcano Rapid Response Balloon Campaign during the 2018 Kilauea

530 Eruption, *Bull. Am. Meteorol. Soc.*, 101, E1602–E1618, <https://doi.org/10.1175/BAMS-D-19-0011.1>, 2020.